Directed Evolution of Rubisco in *Escherichia coli* Reveals a Specificity-Determining Hydrogen Bond in the Form II Enzyme[†]

Oliver Mueller-Cajar,[‡] Matthew Morell,[§] and Spencer M. Whitney*[,‡]

Molecular Plant Physiology, Research School of Biological Sciences, Australian National University, P.O. Box 475, Canberra, Australian Capital Territory 2601, Australia, and CSIRO Plant Industry, GPO Box 1600, Canberra, Australian Capital Territory 2601, Australia CSIRO Plant Industry

Received May 1, 2007; Revised Manuscript Received September 3, 2007

ABSTRACT: Ribulose 1,5-bisphosphate carboxylase/oxygenase (Rubisco) occupies a critical position in photosynthetic CO_2-fixation and consequently has been the focus of intense study. Crystal-structure-guided site-directed mutagenesis studies have met with limited success in engineering kinetic improvements to Rubisco, highlighting our inadequate understanding of structural constraints at the atomic level that dictate the enzyme's catalytic chemistry. Bioselection provides an alternative random mutagenic approach that is useful for identifying and elucidating imperceptible structure−function relationships. Using the dimeric Form II Rubisco from *Rhodospirillum rubrum*, its gene (*rbc*M) was randomly mutated and introduced under positive selection into *Escherichia coli* cells metabolically engineered to be dependent on Rubisco to detoxify its substrate ribulose 1,5-bisphosphate. Thirteen colonies displaying improved fitness were isolated, and all were found to harbor mutations in *rbc*M at one of two codons, histidine-44 or aspartate-117, that are structurally adjacent amino acids located about 10 Å from the active site. Biochemical characterization of the mutant enzymes showed the mutations reduced their CO_2/O_2 specificity by 40% and decreased their carboxylation turnover rate by 20−40%. Structural analyses showed histidine-44 and aspartate-117 form a hydrogen bond in *R. rubrum* Rubisco and that the residues are conserved among other Form II Rubiscos. This study demonstrated the utility of directed evolution in *E. coli* for identifying catalytically relevant residues (in particular nonobvious residues disconnected from active site residues) and their potential molecular interactions that influence Rubisco's catalytic chemistry.

Ribulose 1,5-bisphosphate carboxylase/oxygenase (Rubisco[1]) catalyzes the reaction responsible for virtually all global CO_2 assimilation into biomass. Rubisco's influential role on the global carbon economy stems from its positioning in the gateway between the inorganic and organic phases of the carbon cycle (*1*, *2*). This important role contrasts with the catalytic shortcomings of Rubisco that have resulted in it being a popular target for structure−function studies that might ultimately be useful in engineering more efficient versions for increasing photosynthetic carbon assimilation (*3*). Rubisco is both sluggish, carboxylating its pentose substrate ribulose-P_2 at a rate of 2−13 s^{-1} to produce two molecules of 3-phosphoglycerate (3-PGA), and lacks specificity, oxygenating ribulose-P_2 to produce a molecule each of 3-PGA and 2-phosphoglycolate (2-PG). While 3-PGA is metabolized to triose phosphate by the photosynthetic carbon reduction cycle, 2-PG is considered a waste product since its recycling necessitates the photorespiratory carbon oxidation cycle that recycles only three-quarters of the carbon incorporated into 2-PG and wastes metabolic energy (*4*). The ability of Rubisco to discriminate between the substrates CO_2 and O_2 is given by the specificity constant $S_{c/o} = (k^c_{cat}/K_c)/(k^o_{cat}/K_o)$, which represents the ratio of the enzyme's carboxylation efficiency (carboxylation rate (k^c_{cat}) divided by the K_m for CO_2 (K_c)) to oxygenation efficiency (oxygenation rate (k^o_{cat}) divided by the K_m for O_2 (K_o)) at equal CO_2 and O_2 concentrations (*5*).

All Rubiscos share a common ancestor (*6*) and therefore possess a conserved catalytic mechanism and active site conformations that are virtually superimposable (*7*, *8*). There are, however, significant differences in the kinetic properties and quaternary structures of Rubiscos from different phylogenies. Three distinct forms of Rubisco have been described, all of which contain dimers of large (L, ∼50−53 kDa) subunits that contain the catalytic site (*7*). Form I enzymes, which tend to possess high $S_{c/o}$ values (∼40−170), form a hexadecamer consisting of eight L and eight small (S, ∼13−16 kDa) subunits and are found in land plants, algae, bacteria, and cyanobacterial (*9*). Form II Rubiscos contain only L subunits and are found in some photosynthetic proteobacteria, chemoautotrophic bacteria, and certain dinoflagellate algae (*6*). These Rubiscos tend to feature high k^c_{cat} values but are relatively poor at distinguishing between the gaseous substrates ($S_{c/o}$ ∼ 10−20) (*10*, *11*). The more

[†] This research was supported by Australian Research Council Grants DP0450564 and LP0347461.

* To whom correspondence should be addressed. Tel.: +61-2-6125-5073. Fax: +61-2-6125-5075. E-mail: spencer.whitney@anu.edu.au.

[‡] Australian National University.

[§] CSIRO Plant Industry.

[1] Abbreviations: carboxyarabinitol-P_2, 2′-carboxyarabinitol-1,5-bisphosphate; EPPS, *N*-[2-hydroxyethyl]piperazine-*N*′-3-propanesulfonic acid; fructose-P_2, fructose-1,6-bisphosphate; IPTG, isopropyl-β-D-thiogalactopyranoside; PAGE, polacrylamide gel electrophoresis; ribulose-P_2, D-ribulose-1,5-bisphosphate; Rubisco, ribulose-P_2 carboxylase/oxygenase; SDS, sodium dodecyl sulfate.

10.1021/bi700820a CCC: $37.00
Published on Web 11/16/2007

recently described Form III Rubiscos found in Archeae species can form novel decameric structures that comprise a pentagonal ring of L dimers (*12*).

An abundance of crystallographic and biochemical studies has led to a detailed understanding of the Rubisco reaction mechanism and many of its structure−function relationships (*7*, *8*). These expansive analyses have recently culminated in a synthesis which proposes a thermodynamic rationale for Rubisco's kinetic limitations (*13*), possibly explaining the limited success in engineering more efficient versions by site-directed mutagenesis that have inevitably led to improvements in one or more kinetic properties occurring at the detriment of others (reviewed in refs *1*, *14*).

More recently, the high transformation efficiencies of *Escherichia coli* (up to 10^{10} transformants/μg plasmid) has been used in directed evolution experiments to sample sequence diversity to evolve Form I Rubisco from the cyanobacterium *Synechococcus* PCC6301 (*15*). This study demonstrated the ability to metabolically engineer *E. coli* toward Rubisco dependency, based on alleviating the toxicity of ribulose-P_2 introduced into the cells following transformation with phosphoribulokinase (PRK) (*16*). The *Synechococcus* PCC6301 Rubisco was evolved toward improved fitness in the *E. coli* system, resulting in the isolation of three variant Rubiscos that each contained a Met-259-Thr mutation in the L subunit that improved functional assembly of the enzyme in *E. coli* by >5-fold and modestly improved its catalytic efficiency (*17*).

Here we apply a comparable *E. coli* selection system to evolve the Form II Rubisco from *Rhodospirillum rubrum* toward an improved fitness in a novel physiological context. Structural and kinetic analysis of the evolved variants revealed a previously unexplored conserved hydrogen bond that is functionally linked to sustaining CO_2/O_2 specificity thus establishing directed evolution of Rubisco in *E. coli* as a useful tool for investigating structure−function relationships in the enzyme.

EXPERIMENTAL PROCEDURES

Transformation and Growth of E. coli. Strains XL1-Blue (Stratagene), DH10B, and RR1 (a *rec*A^+ derivative of HB101 that contains the allelic mutations *ara*-14 and *leuB*6 resulting in a proline and leucine auxotrophic phenotype) transformed with plasmids were grown in Luria−Bertani (LB) media containing the requisite antibiotic (ampicillin, 200 μg mL^{-1}; kanamycin, 30 μg mL^{-1}; chloramphenicol, 34 μg mL^{-1}). Following transformation of the *E. coli* strain MM1 (a Δ*gap*A::Km^r mutated RR1 strain, see below) the cells were incubated for 1 h at 37 °C in permissive medium (M9 minimal media containing glycerol (0.4% v/v), malate (0.4% w/v), and cas amino acids (0.4% w/v)) before centrifuging (8000*g*, 1 min), removing all the liquid media by aspiration before suspending the cells in saline solution (0.9% NaCl (w/v)) and plating on agar solidified (1.5% w/v) permissive media.

Plasmid Construction. Detailed procedures for the construction of plasmids are provided in Supporting Information. Plasmid pTrcrbcM contains the *R. rubrum* Rubisco gene (*rbc*M; also known as *cbb*M (*6*)) from pRR1 (*10*) cloned downstream of the *trc* promoter in plasmid pTrcZαSTOP. The first five codons in the *R. rubrum* Rubisco N-terminal coding sequence (MDQSS) are changed to MAMITPSL. Plasmid pTrcK191M encodes a nonfunctional Lys-191-Met Rubisco mutant, and pAC^{BAD}PRK contains the *Synechococcus* PCC7942 *prk*A gene from plasmid pETS7PRK (*18*) cloned into pACYC184 under the control of the *BAD* promoter (P_{BAD}). Plasmids pTrcH44Q, pTrcD117H, and pTrcD117V correspond to clones pBAD0.25D, pBAD0.1A, and pBAD0.1C, respectively, and pTrcH44N contains only the H44N mutation in *rbc*M from clone pBAD0.1B (Table 1). All cloned and selected DNA sequences were fully sequenced using BigDye terminator sequencing (Applied Biosystems) on an ABI 3730 sequencer (Biomolecular Resource Facility, JCSMR, ANU).

Table 1: *R. rubrum* Rubisco Variants Evolved in the MM1-pAC^{BAD}PRK Cells

mutant pBAD clone[a]	evolved amino acid mutations					silent changes to *rbc*M
	H44N	H44Q	D117H	D117V	others	
0.25H	×				S462C	2
0.1B	×				P237S	
0.1E	×				V457A	1
0.25B		×				2
0.25D#		×				
0.25E#		×				
0.25G		×			R428L	
0.1A*			×			
0.25F#			×			
0.1C				×		
0.25A				×	P465L	1
0.25C				×		1
0.1D				×		1

[a] The asterisk (*) and the pound sign (#) indicate identical rbcM sequences.

Error-Prone PCR Amplification of rbcM Genes and the Construction of Plasmid Libraries. The *rbc*M gene in plasmid pTrcrbcM was amplified under different stringency conditions using the primers Trc5 (5′-GAGGTATATAT-TAATGTATCG-3′) and Trc3 (5′-ATCTTCTCTCATCCGC-CA-3′) that anneal to the vector sequence on either side of the pTrcHisB multiple cloning site. On the basis of the method described in ref *19*, each amplification reaction (50 μL final volume) contained 5 U recombinant Taq DNA polymerase (Invitrogen), 1× PCR buffer, 2 ng of plasmid template, 12 pmol of each primer, 0.2 mM of each dNTP, and 1.5 mM $MgCl_2$. The error rate of the amplification reaction was enlarged by increasing the amount of 10xM mutagenic buffer (8 mM dTTP, 8 mM dCTP, 48 mM $MgCl_2$, and 5 mM $MnCl_2$) added. The cycling conditions were one cycle at 95 °C (2 min) then 25 cycles at 95 °C (30 s), 50 °C (30 s), and 72 °C (2 min). PCR products were purified using the Wizard SV PCR and gel cleanup system (Promega), digested with *Hind*III and *Eco*RI, cloned into pTrcZαSTOP, and transformed into electrocompetent DH10B cells. The transformation reactions were diluted 10-fold into LB-ampicillin liquid media and grown overnight at 37 °C. Plasmid DNA was prepared to produce supercoiled plasmid libraries.

Growth of E. coli under Rubisco-Dependent Conditions. The Rubisco-coding plasmids (including the super-coiled plasmid libraries) were transformed into electrocompetent MM1-pAC^{BAD}PRK cells and washed with 0.9% (w/v) NaCl before plating 95% of the cells on selective media (M9 media

supplemented with 0.4% (v/v) glycerol, 0.05% (w/v) cas amino acids, 0.5 mM IPTG, and 0.05% or 0.075% L-arabinose) and 5% on malate-free permissive media (to assess the transformation efficiency) both containing ampicillin and chloramphenicol. Selective plates were incubated at 23 °C in air or in air supplemented with CO_2 (CO_2 levels maintained at ~2% (v/v) using a Vaisala infrared gas analyzer controller) while permissive plates were incubated at 37 °C overnight in air.

R. rubrum Rubisco Expression Analysis. Rubisco content was measured in pTrcrbcM (mutated and nonmutated) transformed MM1 colonies actively growing on selective media or XL1-Blue cells grown in LB-ampicillin liquid media. Scrapings of the MM1 cells were suspended in extraction buffer (100 mM EPPS-NaOH pH 8.0, 1 mM EDTA, 0.05% (w/v) *E. coli* protease inhibitor cocktail (Sigma)), their OD_{600} measured and diluted to equivalent cell densities before lysing with a french pressure cell (140 MPa). The soluble cellular protein was collected by centrifugation (10 min, 16000*g*, 4 °C), and aliquots were either mixed with SDS buffer for SDS PAGE analysis (*20*) or used to measure protein content using the dye-binding Pierce Coomassie Plus kit. Samples were run on duplicate SDS-gels and either stained with Coomassie blue to confirm equal protein loading or blotted onto nitrocellulose, and *R. rubrum* Rubisco expression was analyzed using antibodies to pure *Symbiodinium* Form II Rubisco as described previously (*21*). Rubisco content in the XL1-Blue extracts was quantified by [2-^{14}C]carboxyarabinitol-P_2 inhibitor binding after preincubation with 40 mM $NaHCO_3$ and 20 mM $MgCl_2$ as described (*22*). Purified [2-^{14}C]carboxyarabinitol-P_2 was synthesized according to ref *23*. The binding assays were done in duplicate and incubated for 20 min with 15 or 45 μM [2-^{14}C]-carboxyarabinitol-P_2 at 25 °C with the same amount of Rubisco-bound-[2-^{14}C]carboxyarabinitol-P_2 recovered by gel filtration in both assays, indicating tight binding to both the wild-type and mutated *R. rubrum* Rubiscos.

Ribulose-P_2 Quantification. Scrapings of similarly sized colonies of MM1-pAC^{BAD}PRK cells transformed with pTrcrbcM (13 days) or mutant plasmids (9 days) actively growing on plates of selective media (0.05% (w/v) arabinose) were suspended in 1.5 mL of extraction buffer, and 1 mL was rapidly frozen by mixing with 2 mL of 75% (v/v) methanol chilled to −80 °C. The frozen cells were harvested by centrifugation (6000*g*) for 5 min at −10 °C. Frozen cell pellets were resuspended in 5% (v/v) trifluoroacetic acid, sonicated for 10 s to complete lysis, and centrifuged at 4 °C (13000*g*, 5 min), and the supernatant was collected and dried with a gentle stream of N_2. The dried residue was dissolved in 200 μL of water, and ribulose-P_2 content was measured using $NaH^{14}CO_3$ assays. The cell number of the unfrozen cells was determined from absorbance (OD_{600}) measurements and used to calculate cellular ribulose-P_2 concentration as described previously (*16*) knowing 3.6×10^7 RR1 cells mL^{-1} have an OD_{600} of 0.5.

Rubisco Extraction, Purification, and Thermal Stability Analysis. Plasmids expressing wild-type and mutated *R. rubrum* Rubiscos were transformed into XL1-Blue and grown in 1 L LB-ampicillin at 37 °C, and at a OD_{600} of ~0.6 Rubisco production was induced with 0.5 mM IPTG for 6 h before harvesting by centrifugation (5 min at 6000*g*). The cells were suspended in extraction buffer and lysed with a French pressure cell (140 MPa), and the Rubiscos were purified as described in ref *24*. The thermal stability of each enzyme was measured by differential scanning calorimetry (DSC) using a VP-DSC calorimeter from MicroCal Corporation (Northampton, MA). The cell volume was 0.51 mL, and the enzymes were dialyzed into 2 L of DSC buffer (20 mM Hepes-NaOH, 50 mM NaCl, 0.5 mM EDTA, 20% glycerol, pH 8) and diluted to final concentrations of 1.2 μM. Values of the apparent temperature of unfolding, T_u, were obtained from DSC unfolding peaks of upward scans (using a scan rate of 90 K h^{-1}) using the DSC in Origin software.

Rubisco Kinetics. The purified Rubisco preparations were used to measure the Michaelis constants for substrates CO_2 (K_c) and ribulose-P_2 (K_{RuBP}) at 25 °C, pH 8, using $^{14}CO_2$-fixation assays according to ref *20*. Ribulose-P_2 was synthesized and purified as described ref *25*. The Rubiscos were preactivated for 30 min with 20 mM $MgCl_2$ and 40 mM $NaHCO_3$ before assaying for activity. The data was fitted to the Michaelis−Menten equation and the catalytic turnover rate (k^c_{cat}) was calculated from the K_c measurements made under nitrogen by dividing the extrapolated maximal carboxylase activity by the concentration of Rubisco active sites in the assay quantified by [2-^{14}C]carboxyarabinitol-P_2 inhibitor binding (*22*) and stoichiometric binding of the inhibitor confirmed by comparative immunoblot analysis (see above) of the purified enzymes. The CO_2/O_2 specificity ($S_{c/o}$) was measured in reactions equilibrated with an atmosphere of O_2 accurately mixed with 0.5% (v/v) CO_2 using Wösthoff pumps at pH 8.3 as described in ref *26*. As both oxygen and fructose-P_2 are competitive inhibitors with regard to Rubisco carboxylation and ribulose-P_2 fixation, respectively, the K_c measurements were made at different oxygen concentrations (0, 10, and 20% (v/v) oxygen mixed with nitrogen using Wösthoff pumps) and K_{RuBP} was measured in the presence of 0, 120, and 240 μM fructose-P_2. The inhibition constants (K_I) for O_2 (K_o) and fructose-P_2 (K_I(FBP)) were then calculated by fitting the data to the equation $K_m^{app} = K_m(1 + I/K_I)$ where I is the inhibitor concentration and K_m^{app} is the measured K_m at different inhibitor concentrations.

RESULTS

A High-Throughput Selection System for Rubisco Activity in E. coli. The concept of Rubisco-dependent *E. coli* was first proposed by our laboratory (*27*) and was based on coexpression of phosphoribulokinase (PRK) and Rubisco in a glycolytic deletion mutant where the *gap*A gene (coding glyceraldehyde-3-phosphate dehydrogenase) has been removed. Introducing a metabolic shunt consisting of PRK and Rubisco was predicted to complement the Δ*gap*A mutation, thus resulting in *E. coli* that were dependent on Rubisco (and PRK) expression when grown on minimal media containing a carbon source (such as glycerol) upstream of the glycolytic lesion. However, despite numerous attempts an MM1 Δ*gap*A strain (derived by insertional inactivation of *gap*A in the proline/leucine auxotrophic *E. coli* strain RR1 that is a *rec*A$^+$ derivative of HB101, see Experimental Procedures) expressing spinach PRK and *R. rubrum* Rubisco could not grow under selective conditions on M9 media containing glycerol, leucine, and proline (Morell, 1990 unpublished data). Recent re-examination of the selection system found that the toxicity induced by ribulose-P_2 build-up following PRK expression

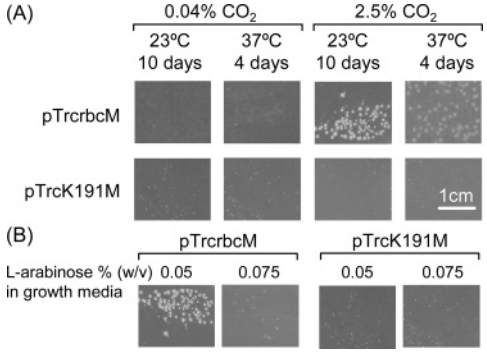

FIGURE 1: Rubisco-dependent *E. coli* selection. (A) MM1-pAC^{BAD}-PRK cells were transformed with pTrcrbcM and pTrcK191M (encoding functional and nonfunctional *R. rubrum* Rubisco, respectively) and plated on selective media (M9 media containing 0.4% v/v glycerol, 0.05% w/v casamino acids, 0.5 mM IPTG, and 0.05% L-arabinose). Growth was only observed if the cells were transformed with functional Rubisco and plated out at elevated levels of CO_2. (B) Inability of MM1-pAC^{BAD}PRK-pTrcrbcM cells to grow on selective media containing 0.075% (w/v) L-arabinose after 10 days at 23 °C in air supplemented with 2% (v/v) CO_2.

in *E. coli* (*16*) could be alleviated by coexpressing bacterial Rubiscos at elevated levels of CO_2 and supplementing the growth media with limiting concentrations of casamino acids, analogous to that recently observed (*15*).

Coexpression of PRK and Rubisco in the MM1 (Δ*gap*A::Km^R) and its parental RR1 *E. coli* strains used a two-plasmid system that was comprised of a pACYC184-based plasmid (pAC^{BAD}PRK), encoding *Synechococcus* PCC7942 PRK under the control of the L-arabinose inducible BAD promoter (*28*), and pTrcHisB-based plasmids containing *Rhodospirillum rubrum* Rubisco gene (*rbc*M) variants that coded for functional enzyme (pTrcrbcM) or a mutated *rbc*M (pTrcK191M). pTrcK191M codes for inactive enzyme due to a mutation at the catalytically essential active site lysine residue at codon 191 that is required to bind nonsubstrate CO_2 to form a carbamate that initiates Mg^{2+} binding thus 'activating' the active site for catalysis (*8*). Contrary to that expected, the growth of small colonies were observed when RR1-pAC^{BAD}-PRK cells transformed with pTrcK191M were grown on selective media (M9 media supplemented with 0.4% v/v glycerol, 0.05% (w/v) cas amino acids, 0.5 mM IPTG, and 0.05% (w/v) L-arabinose) in air or air supplemented with 2% (v/v) CO_2 (data not shown). Similar false positives were also reported (*15*) using the wild-type *E. coli* strain K12 that effectively limited the number of cells that could be effectively screened on a agar plate to $\sim 10^4$ colony forming units (cfu). Interestingly, no false positives were observed for MM1-pAC^{BAD}PRK-pTrcK191M cells grown on selective media at either CO_2 level. In fact, MM1-pAC^{BAD}PRK colonies only grew on selective media when transformed with a plasmid encoding functional Rubisco and incubated at elevated levels of CO_2 (Figure 1A). Consequently MM1 was a preferred host for the Rubisco-dependent *E. coli* system and allowed plating of very large numbers of transformants ($\sim 3 \times 10^5$ cfu) per agar plate.

Modulating the Sensitivity to Rubisco Fitness in MM1. Screening for changes in the catalytic fitness of Rubisco in MM1-pAC^{BAD}PRK cells was achieved by adjusting the concentration of L-arabinose (which induced PRK expression) in the growth media. The *ara*-14 mutation in MM1, which prevents metabolism of L-arabinose, was expected to avert uneven induction of the pBAD promoter (*28*) and thereby enable accurate modulation of PRK production in the MM1-pAC^{BAD}PRK cells using varying inducer (L-arabinose) concentrations. On selective media containing 0.05% (w/v) L-arabinose, MM1-pAC^{BAD}PRK cells transformed with pTrcrbcM (encoding *R. rubrum* Rubisco) were able to form colonies after 10 days at 23 °C in air containing 2% (v/v) CO_2 but not at slightly higher L-arabinose (0.075% (w/v) concentrations (Figure 1B). In replicate experiments performed at 37 °C, the MM1-pAC^{BAD}PRK cells transformed with pTrcrbcM were able to grow at higher inducer concentrations (0.2% (w/v) L-arabinose) after 4 days, indicating the slower growing cells at 23 °C appeared more sensitive to the selection pressure than those grown at 37 °C.

Directed Evolution of R. rubrum Rubisco. Using the selective condition where the *R. rubrum* Rubisco was unable to support growth in MM1-pAC^{BAD}PRK cells (i.e., on selective media containing 0.075% (w/v) L-arabinose at 23 °C, Figure 1B), the enzyme was evolved toward an improved fitness in this novel physiological context. Two supercoiled plasmid libraries of the *rbc*M gene were generated using error-prone PCR at two different mutagenic stringencies (see Experimental Procedures) and designated 0.1x M*rbc*M and 0.25x M*rbc*M (containing 190 000 and 288 000 library members, respectively). These were transformed into electrocompetent MM1-pAC^{BAD}PRK cells, and $\sim 10^5$ cells from each library were plated on selective media containing 0.075% (w/v) L-arabinose. Five percent of the transformation was plated on permissive media (selective media without L-arabinose) and formed a confluent cell lawn. On the selective media, 5 and 20 colonies from the 0.1x M*rbcM* and 0.25x M*rbcM* transformed cells, respectively, had formed after 10 days. The pTrcrbcM plasmids from the 0.1x M*rbcM* colonies (designated pBAD0.1A−E) and eight of the 0.25x M*rbcM* colonies (designated pBAD0.25A−H) were isolated, and the *rbc*M was sequenced. Mutation rates of approximately 1.1×10^{-3} and 1.3×10^{-3} were calculated for the 0.1x M*rbcM* and 0.25x M*rbcM* libraries, respectively, with all the clones having a mutation either at the codon for histidine-44 or aspartate-117 (summarized in Table 1). The His-44 had mutated to the amide functionalities of asparagine (H44N) or glutamine (H44Q), and Asp-117 was mutated to either histidine (D117H) or valine (D117V). Apart from clones pBAD0.25D and pBAD0.25E, all mutants were derived from different PCR products since they contained unique substitutions in their *rbc*M sequence or the same mutation originated from different libraries (for example, clones pBAD0.1A and pBAD0.25F).

To confirm the mutations at codons His-44 and Asp-117 imparted the improvement in fitness, pTrcrbcM variants containing single *rbc*M mutations that coded for the H44N, H44Q, D117H, or D117V mutations were retransformed into MM1-pAC^{BAD}PRK. Unlike the wild-type control, the evolved Rubisco variants were able to support growth on selective media containing 0.075% (w/v) arabinose (Figure 2A). This suggested that the other observed mutations (both silent and nonsilent, Table 1) were not the primary determinants for the improvement in fitness of the evolved *R. rubrum* Rubiscos.

Biochemical and Biophysical Characterization of the Selected Mutants. Possible mechanisms by which the evolved Rubisco variants might improve the tolerance of the *E. coli*

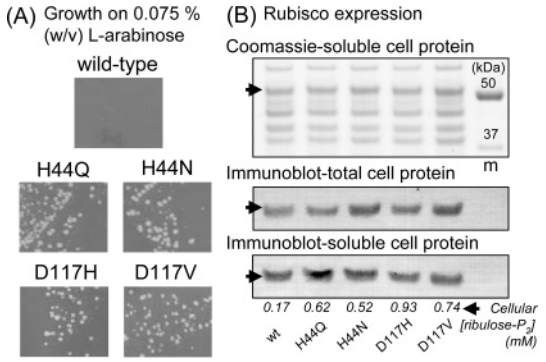

FIGURE 2: (A) Growth after 10 days on selective media containing 0.075% (w/v) L-arabinose at 23 °C in air supplemented with 2% (v/v) CO_2 of MM1-pAC^{BAD}PRK cells transformed with pTrcrbcM-based plasmids coding wild-type and mutated *R. rubrum* Rubisco that contain glutamine and asparagine substitutions at histidine-44 (H44Q, H44N) or histidine and valine substitutions at aspartate-117 (D117H, D117V). (B) SDS-PAGE and immunoblot analysis of wild-type and mutant *R. rubrum* Rubisco expression (arrow) in the total and soluble cellular protein from 2.2×10^6 MM1-pAC^{BAD}-PRK transformed cells actively growing on selective media containing 0.05% (w/v) L-arabinose. The corresponding ribulose-P_2 cellular concentrations are shown in italics. m, molecular weight marker with sizes shown.

to ribulose-P_2 toxicity include improvements in the relative stability or level of functional *R. rubrum* Rubisco produced in the cells. Using purified enzyme, DSC scans of the heat-induced unfolding showed the apparent temperatures of unfolding (T_u) were comparable for the mutant (H44N, 73.2 °C; H44Q, 72.3 °C; D117V, 72.7 °C; D117H, 72.8 °C) and wild-type (72.9 °C) *R. rubrum* Rubiscos indicating the conformational folding and intrinsic stability of mutant Rubiscos were similar to those of the wild-type. Immunoblot analysis of the total and soluble cellular protein from MM1 cells actively growing on selective media showed the mutant and wild-type *R. rubrum* Rubisco produced in vivo was soluble and accumulated to similar levels in the *E. coli* (Figure 2B,C). Likewise, both immunoblot and [2-^{14}C]-carboxyarabinitol inhibitor binding analyses showed the expression level of the Rubisco mutant proteins in XL1-Blue *E. coli* cultured in LB liquid media were the same as, or not more than 40% lower than, the wild-type enzyme that accumulated to ~3% of the total soluble cellular *E. coli* protein. This indicated the observed improvement in fitness was not due to an increase in the amount of functional Rubisco produced in the MM1 cells.

Using purified enzyme the kinetic properties of the H44N, D117V, D117H, and H44Q Rubisco variants were measured in a bid to identify the mechanism(s) by which they were selected. Compared with wild-type *R. rubrum* Rubisco, all four evolved variants showed ~40% reductions in $S_{c/o}$, indicating they were identically impaired in their ability to discriminate between CO_2 and O_2 (Table 2). The carboxylase turnover (k^c_{cat}) of the Rubisco variants was also impaired relative to wild-type, showing ~40% and 22% decreases for the Asp-117 and His-44 mutants, respectively. The apparent affinity for CO_2 was additionally perturbed by the mutations resulting in higher Michaelis constants (K_m) for CO_2 (K_c) for the mutant Rubiscos, in particular the H44Q mutant. In contrast the measured K_o (K_m for O_2) values indicated no change for the D117V mutant and only modest differences for the remaining three Rubisco variants. Calculations of k^o_{cat} indicated the oxygenation rate of the four variant Rubiscos were equivalent or slower than wild-type *R. rubrum* Rubisco. The mutant Rubiscos also had little (<25%) or no change in their apparent K_M for ribulose-P_2 $K^{(app)}_{RuBP}$ and were more susceptible to competitive inhibition by fructose 1,6-bisphosphate (FBP) (*29*) than the wild-type enzyme (i.e., lower K_I(FBP) values, Table 2). Taken together, the lower carboxylation (k^c_{cat}/K_c) and oxygenation (k^o_{cat}/K_o) efficiencies of the mutant Rubiscos and equivalent ribulose-P_2 binding affinities indicated their capacity to process ribulose-P_2 was reduced compared to the wild-type. Consistent with this, the cellular ribulose-P_2 concentrations were >3-fold higher in MM1-pAC^{BAD}PRK cells expressing the mutant Rubiscos (~0.5−0.9 mM) compared with those producing the wild-type enzyme (0.17 mM, Figure 2B).

It was reasoned the improved growth rate of the cells expressing the lower specificity Rubiscos may be due to *E. coli* preferring the oxygenation product 2-PG over the carboxylation product 3-PGA. Metabolism of 2-PG in *E. coli* occurs via 2-PG phosphatase (coded by the *gph* gene (*30*)) producing glycolate which can be readily used as a sole carbon source to support cell growth (*31*). To examine this hypothesis a Δ*gph E. coli* mutant (strain JW3348 from the Keio collection (*32*)) was transformed with pAC^{BAD}PRK and the variant Rubisco genes, and their growth on selective solid media containing varying levels of L-arabinose (inducer of PRK) were compared against similarly transformed wild-type RR1 cells. In cells producing just Rubisco, the relative growth of both *E. coli* strains on LB containing 0.5 mM IPTG were unvaried. However differences in colony growth were observed between the strains with the inclusion of PRK. Analogous to MM1 cells, the mutant Rubiscos conferred a growth advantage to RR1-pAC^{BAD}PRK cells on selective media (0.025% (w/v) arabinose, 0.5 mM IPTG) and grew faster and indifferently on permissive media (Figure 1 in Supporting Information). In contrast, the growth of the JW3348-pAC^{BAD}PRK cells producing wild-type or mutant Rubiscos were similarly constrained on permissive media (and on nutrient-rich LB media, data not shown) and totally impeded on media containing minimal levels of L-arabinose (0.025% w/ v) (Figure 1B in Supporting Information). This sensitivity to PRK and Rubisco production precluded the discrimination of any growth variation between the Δ*gph*-PRK cells producing either wild-type or mutant Rubiscos. In some plating experiments colonies of JW3348-pAC^{BAD}-PRK-Rubisco producing cells grew normally on selective media and even on media containing 0.05% (w/v) L-arabinose (data not shown). Consistent with their sensitivity to PRK-Rubisco production it was shown by restriction analyses of pAC^{BAD}PRK from these cells that PRK production had been disrupted by inclusion of transposons within the *prk* coding region (data not shown). This alleviation of PRK production by transposon inactivation was not unique to JW3348 and was also observed in pAC^{BAD}PRK-pTrcrbcM transformed RR1 and XL1Blue *E. coli* cells grown on nonpermissive selective media containing 0.075% (w/v) L-arabinose but never observed in MM1 cells under any selective condition (data not shown).

DISCUSSION

We describe the application of a high-throughput *E. coli* selection that successfully yielded an array of reproducible

Table 2: Kinetic Parameters of Wild-Type and Evolved *R. rubrum* Rubiscos

Rubisco	$S_{c/o}$ ($k_c^{cat}K_o/k_o^{cat}K_c$)	k_c^{cat} (s^{-1})[a]	K_c (μM)	K_o (μM)	k_o^{cat} (s^{-1})[b]	k_c^{cat}/K_C (s^{-1} mM^{-1})	k_o^{cat}/K_o (s^{-1} mM^{-1})	$K_r^{(app)}$ (μM)	K_I(FBP) (μM)
wild-type	9.0 ± 0.3	12.3 ± 0.3	149 ± 8	159 ± 25	1.4	83	8.9	63 ± 2	465 ± 70
D117V	5.3 ± 0.1	7.4 ± 0.3	196 ± 18	199 ± 51	1.5	38	7.6	55 ± 6	347 ± 83
D117H	5.3 ± 0.1	7.5 ± 0.2	192 ± 10	153 ± 35	1.1	39	7.3	48 ± 8	245 ± 64
H44Q	5.3 ± 0.1	9.3 ± 0.6	301 ± 38	185 ± 58	1.2	31	6.4	56 ± 14	348 ± 40
H44N	5.5 ± 0.3	9.8 ± 0.4	204 ± 18	116 ± 25	1.0	48	8.8	59 ± 11	320 ± 92

[a] Rate calculated from maximal carboxylase activity extrapolated from the Michaelis−Menten fit from K_c measurements. [b] Rate calculated from the equation $S_{c/o} = (k_{cat}^c/K_c)/(k_{cat}^o/K_o)$ (*36*).

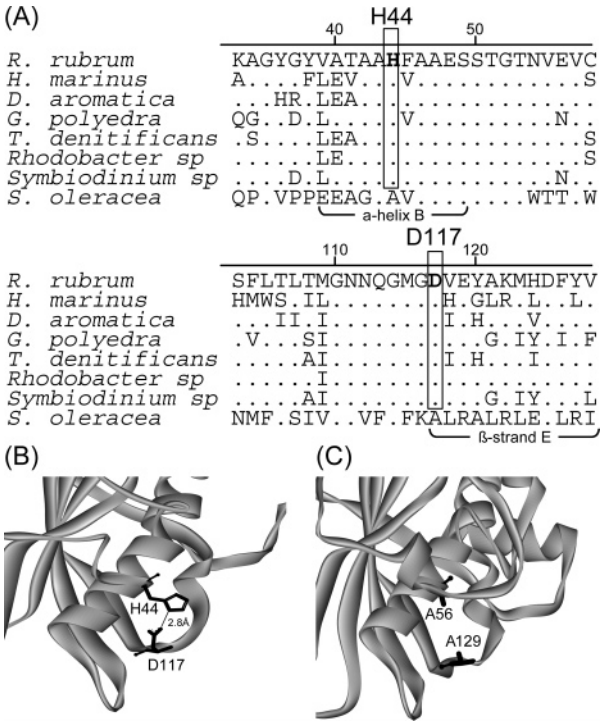

FIGURE 3: Conservation and location of histidine-44 (His-44) and aspartate-117 (Asp-117) in *R. rubrum* Rubisco. (A) Partial sequence alignment around the *R. rubrum* His-44 (H-44) and Asp-117 (D117) residues (in bold and boxed) with six Form II and one Form I (spinach; *S. oleracea*, GenBank accession no. P00875) Rubisco sequences. Only residues differing from the *R. rubrum* sequence are shown. GenBank accession nos. for Rubisco sequences are as follows: *R. rubrum*, YP_427487; *Hydrogenovibrio marinus*, BAD15326; *Dechloromonas aromatica*, YP_286836; *Gonyaulax polyedra*, GONR15B; *Thiobacillus dentirificans*, YP_316396; *Rhodobacter sphaeroides*, EAP66890 or *R. capsulatus*, AAB82048; *Symbiodinium* sp., AAG37859. (B) Structure of one L subunit from nonsubstrate bound *R. rubrum* Rubisco (PDB code 5RUB) showing the structural hydrogen bond between His-44 and Asp-117 (*37*) that is not present in (C) the L subunit of spinach Form I Rubisco where the corresponding residues are Ala-56 and Ala-129 (*38*) (PDB code 8RUC). Structures were assembled using DS viewer Pro software.

Form II *R. rubrum* Rubisco variants that contained mutations at either His-44 or Asp-117 that displayed quasi-identical kinetics (Tables 1 and 2). A comparison with other Rubisco L sequences showed that the residues are both found in the N-terminal domain of the L subunit and are conserved in Form II enzymes but not in the hexadecameric Form I where the corresponding residues tend to be alanine (*33*) (Figure 3A). Examination of the L_2 quaternary structure of *R. rubrum* Rubisco showed both residues are located adjacent to each other and are positioned within 10 Å of the bound ribulose-P_2 substrate. Closer examination of the available Rubisco crystal structures revealed the residues form a hydrogen bond in *R. rubrum* Rubisco with the hydrogen bound to the imidazole nitrogen of His-44 acting as donor, and a carboxyl oxygen of Asp-117 being the acceptor (Figures 3B and 4). This hydrogen bond is absent in the corresponding Form I Rubiscos (Figure 3C).

In the *R. rubrum* enzyme His-44 is positioned in the center of α-helix B which contains a completely conserved, and catalytically essential, glutamate residue (Glu-48; terminology of strands and helices follows (*34*)). Asp-117 is located on the N-terminal end of *β*-strand E (Figure 3). During catalysis, the gas addition reaction of Rubisco is mediated via a catalytically essential lysine (Lys-329) that is located at the apex of the flexible loop 6 that 'closes' over the active site during catalysis. The amine functionality of Lys-329 is thought to polarize the oxygen atoms of substrate CO_2 making the carbon more electrophilic and susceptible to nucleophilic attack from the enediol intermediate (*1*, *8*). In the 'closed' form of the enzyme, Glu-48 forms a salt bridge with Lys-329, presumably ensuring its correct positioning during loop-closure (*1*, *8*, *35*). It thus seems likely that the loss of the structural hydrogen bond between His-44 and Asp-117 in *R. rubrum* Rubisco, as brought about by the selected mutations, may sufficiently alter the positioning of Glu-48, thereby affecting loop closure and the positioning of Lys-329. This is consistent with the observed reductions in $S_{c/o}$ and k_{cat}^c in the evolved variant enzymes (Table 2) since previous studies have shown that mutations that affect the positioning of Lys-329 have led to reductions in both parameters (*1*, *14*). The apparent importance of the His-44/Asp-117 hydrogen bond to the CO_2/O_2 specificity may explain the conservation of these residues in Form II Rubiscos since, although characteristically having low $S_{c/o}$ values, a further decline in the ability of a Form II Rubiscos to discriminate between CO_2 and O_2 may be detrimental to the survival of their natural hosts.

Despite all the isolated *R. rubrum* Rubiscos sharing quasi-identical biochemical properties, it remains unclear as to how this clearly defined biochemical phenotype imparts an improved fitness compared to the wild-type enzyme in the MM1-pAC^{BAD}PRK cells. On the basis of our current understanding of the selection system, an increased capability for the detoxification of ribulose-P_2 should confer increased fitness. However, on the basis of the in vitro kinetic measurements made with purified enzyme, the isolated mutants did not meet this requirement. Both the carboxylation and the oxygenation efficiencies (k_{cat}^c/K_c and k_{cat}^o/K_o, respectively) of all the mutants were less than those of the wild-type, indicating a reduced capacity to process ribulose-P_2 which was supported by higher ribulose-P_2 levels in cells

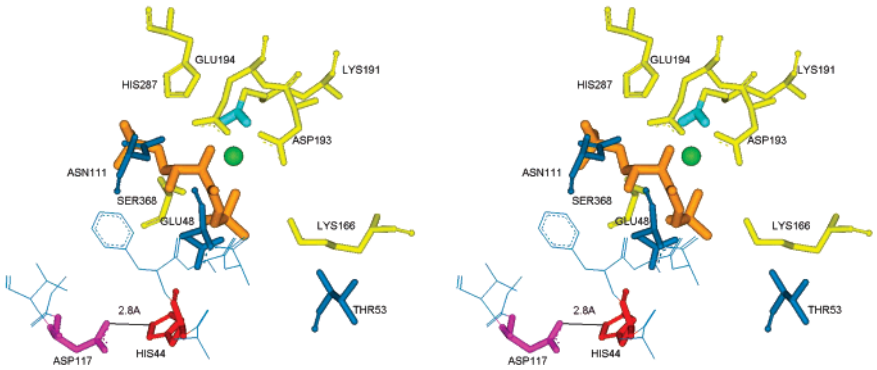

FIGURE 4: Stereoview of the conserved active site residues in *R. rubrum* Rubisco and the relative location of the selected residues (PDB code 9RUB (*39*)). The active site region of every Rubisco is formed between a moiety of the C-terminal (TIM-barrel) domain of one L (yellow residues) and a smaller region of the N-terminal domain of the adjacent L (blue residues) (*7*). To activate the site, nonsubstrate CO_2 binds to the amine group of a lysine (LYS-191, numbering relative to *R. rubrum* Rubisco) to form a carbamate moiety (light blue) which is stabilized by Mg^{2+} (green) binding and enables ribulose-P_2 binding (orange) (*8*). The mutation of ASP-117 or HIS-44 may affect the positioning of glutamate-48 (GLU-48) that influences the positioning of a conserved lysine in loop 6 (LYS-329, not shown as dynamic movement of loop 6 residues precluded their structural resolution) that directs the addition of gaseous substrate to ribulose-P_2 upon catalytic closure of the loop. The orientation of residues between HIS-44 and GLU-48 and those on either side of Asp-117 and His-44 are shown as thin lines.

expressing the mutant enzymes. The lower CO_2/O_2 specificity of the mutants would favor the oxygenation of the ribulose-P_2, resulting in the production of more 2-phosphoglycolate (2-PG) relative to 3-phosphoglycerate (3-PGA) in the cells. If 2-PG can be preferentially metabolized by *E. coli* relative to 3-PGA, then this may serve as the selection pressure by which the mutants were selected, providing an alternative fitness solution in the MM1-pAC^{BAD}PRK selection system other than increasing ribulose-P_2 turnover. In support of this possibility we found the phenotypically normal Δ*gph E. coli* strain JW3348, which cannot make 2-PG phosphatase, was highly sensitive to coexpressing PRK and Rubisco whose production was toxic to growth. While this sensitivity obscured our attempts to show a growth advantage to Δ*gph*-PRK cells producing wild-type Rubisco (hypothetically resulting from a higher proportion of 3-PGA/2-PG produced relative to cells producing the mutated Rubiscos), the sensitivity to 2-PG production associated with the Δ*gph* mutation potentially provides a useful strategy for incorporation into MM1 cells (where false positives due to transposon silencing of PRK production are not selected) to enable screening specifically for Rubisco mutants with improvements in $S_{c/o}$. Such efforts would benefit from a better understanding of the physiological properties that influence Rubisco fitness in MM1, particularly if we are to fully exploit the high genetic diversity that can be screened by heterologous expression in *E. coli* (~5000 cfu per cm^2 of media using MM1-pAC^{BAD}PRK). For example, to increase the throughput of the screening system there is a need to understand why slower growing cells appeared more sensitive to the selection pressure than those grown at 37 °C (Figure 1).

Despite the current MM1-pAC^{BAD}PRK screening system being unable to select for *R. rubrum* Rubisco variants with 'useful' improvements in kinetic fitness, it did successfully demonstrate the utility of using directed evolution to highlight previously unrecognized structure−function relationships and catalytically important residues in Rubisco using an *E. coli* host. Application of this novel tool to screen mutant libraries of different Rubiscos, such as the form I *Synechococcus* PCC 7942 Rubisco that enables the MM1-pAC^{BAD}PRK cells to survive on selective media with higher arabinose levels (data not shown), and screening under different CO_2 and O_2 pressures is expected to yield further interesting mutants that will increase our understanding of Rubisco structure−function relationships as well as providing insight into ways in which the selective pressures within the MM1 host might be manipulated toward selecting for 'useful' traits, such as an increased rate of ribulose-P_2 carboxylation or improved selectivity for CO_2 over O_2.

ACKNOWLEDGMENT

We thank Inger Andersson for valuable comments on the manuscript, John Andrews for his contribution to the research, Jeff Wilson for the photography, Adele Williamson for assistance in acquiring the DSC data, and Akira Wadano for plasmid pETS7PRK. Strain JW3348 was a gift from the National BioResource Project (NIG, Japan): *E. coli*.

SUPPORTING INFORMATION AVAILABLE

Detailed experimental procedures for construction of the transforming plasmids, the Δ*gap*A::Km^r strain MM1, and the comparative growth experiments of RR1- pAC^{BAD}PRK and JW3348-pAC^{BAD}PRK expressing the different Rubiscos. This material is available free of charge via the Internet at http://pubs.acs.org.

REFERENCES

1. Parry, M. A. J., Andralojc, P. J., Mitchell, R. A. C., Madgwick, P. J., and Keys, A. J. (2003) Manipulation of Rubisco: the amount, activity, function and regulation, *J. Exp. Bot. 54*, 1321−1333.
2. Spreitzer, R. J., and Salvucci, M. E. (2002) Rubisco: Structure, regulatory interactions, and possibilities for a better enzyme *Ann. Rev. Plant Biol. 53*, 449−475.
3. Parry, M. J., Madgwick, P. J., Carvalho, J. F. C., and Andralojc, P. J. (2007) Prospects for increasing photosynthesis by overcoming the limitations of Rubisco, *J. Agric. Sci. 145*, 31−43.
4. Wingler, A., Lea, P. J., Quick, W. P., and Leegood, R. C. (2000) Photorespiration: metabolic pathways and their role in stress protection, *Philos. Trans. R. Soc. London, Ser. B 355*, 1517−29.
5. Laing, W. A., Ogren, W. L., and Hageman, R. H. (1974) Regulation of soybean net photosynthetic CO_2 fixation by the interaction of CO_2, O_2, and ribulose 1,5-bisphosphate carboxylase, *Plant Physiol. 54*, 678−685.

6. Tabita, F. R. (1999) Microbial ribulose 1,5-bisphosphate carboxylase/oxygenase: A different perspective, *Photosynth. Res. 60*, 1−28.
7. Andersson, I., and Taylor, T. C. (2003) Structural framework for catalysis and regulation in ribulose-1,5-bisphosphate carboxylase/oxygenase, *Arch. Biochem. Biophys. 414*, 130−140.
8. Cleland, W. W., Andrews, T. J., Gutteridge, S., Hartman, F. C., and Lorimer, G. H. (1998) Mechanism of Rubisco - the carbamate as general base, *Chem. Rev. 98*, 549−561.
9. Watson, G. M. F., and Tabita, F. R. (1997) Microbial ribulose 1,5-bisphosphate carboxylase/oxygenase: A molecule for phylogenetic and enzymological investigation, *FEMS Microbiol. Lett. 146*, 13−22.
10. Morell, M. K., Kane, H. J., and Andrews, T. J. (1990) Carboxylterminal deletion mutants of ribulosebisphosphate carboxylase from *Rhodospirillum rubrum*, *FEBS Lett. 265*, 41−45.
11. Whitney, S. M., and Andrews, T. J. (1998) The CO_2/O_2 specificity of single-subunit ribulose-bisphosphate carboxylase from the dinoflagellate, *Amphidinium carterae*, *Aust. J. Plant Physiol. 25*, 131−138.
12. Kitano, K., Maeda, N., Fukui, T., Atomi, H., Imanaka, T., and Miki, K. (2001) Crystal structure of a novel-type archaeal Rubisco with pentagonal symmetry, *Structure 9*, 473−481.
13. Tcherkez, G. G. B., Farquhar, G. D., and Andrews, T. J. (2006) Despite slow catalysis and confused substrate specificity, all ribulose bisphosphate carboxylases may be nearly perfectly optimized, *Proc. Natl. Acad. Sci. U.S.A. 103*, 7246−7251.
14. Kellogg, E. A., and Juliano, N. D. (1997) The structure and function of Rubisco and their implications for systematic studies, *Am. J. Bot. 84*, 413−428.
15. Parikh, M. R., Greene, D. N., Woods, K. K., and Matsumura, I. (2006) Directed evolution of Rubisco hypermorphs through genetic selection in engineered *E. coli*, *Protein Eng. Des., Select. 19*, 113−119.
16. Hudson, G. S., Morell, M. K., Arvidsson, Y. B. C., and Andrews, T. J. (1992) Synthesis of spinach phosphoribulokinase and ribulose 1,5- bisphosphate in *Escherichia coli*, *Aust. J. Plant Physiol. 19*, 213−221.
17. Greene, D. N., Whitney, S. M., and Matsumura, I. (2007) Artificially evolved *Synechococcus* PCC6301 Rubisco variants exhibit improvements in folding and catalytic efficiency, *Biochem. J. 404*, 517−524.
18. Kobayashi, D., Tamoi, M., Iwaki, T., Shigeoka, S., and Wadano, A. (2003) Molecular characterization and redox regulation of phosphoribulokinase from the cyanobacterium *Synechococcus* sp PCC 7942, *Plant Cell Physiol. 44*, 269−276.
19. Matsumura, I., and Ellington, A. D. (2002) Mutagenic PCR of protein-coding genes for in vitro evolution, in *Methods in Mol. Biol.* (Braman, J., Ed.) pp 261−269, Humana Press, Totowa.
20. Whitney, S. M., and Sharwood, R. E. (2007) Linked Rubisco subunits can assemble into functional oligomers without impeding catalytic performance, *J. Biol. Chem. 282*, 3809−3818.
21. Whitney, S. M., Shaw, D. C., and Yellowlees, D. (1995) Evidence that some dinoflagellates contain a ribulose-1, 5-bisphosphate carboxylase/ oxygenase related to that of the α-proteobacteria, *Proc. Royal Soc. London, Ser. B 259*, 271−275.
22. Whitney, S. M., and Andrews, T. J. (2001) Plastome-encoded bacterial ribulose-1,5-bisphosphate carboxylase/oxygenase (RubisCO) supports photosynthesis and growth in tobacco, *Proc. Natl. Acad. Sci. U.S.A. 98*, 14738−14743.
23. Pierce, J., Tolbert, N. E., and Barker, R. (1980) Interaction of ribulosebisphosphate carboxylase/oxygenase with transition-state analogues, *Biochemistry 19*, 934−942.
24. Andrews, T. J., and Kane, H. J. (1991) Pyruvate is a by-product of catalysis by ribulosebisphosphate carboxylase oxygenase, *J. Biol. Chem. 266*, 9447−9452.
25. Kane, H. J., Wilkin, J. M., Portis, A. R., and Andrews, T. J. (1998) Potent inhibition of ribulose-bisphosphate carboxylase by an oxidized impurity in ribulose-1,5-bisphosphate, *Plant Physiol. 117*, 1059−1069.
26. Kane, H. J., Viil, J., Entsch, B., Paul, K., Morell, M. K., and Andrews, T. J. (1994) An improved method for measuring the CO_2/O_2 specificity of ribulosebisphosphate carboxylase-oxygenase, *Aust. J. Plant Physiol. 21*, 449−461.
27. Morell, M. K., Paul, K., Kane, H. J., and Andrews, T. J. (1992) Rubisco: Maladapted or misunderstood? *Aust. J. Bot. 40*, 431−441.
28. Guzman, L. M., Belin, D., Carson, M. J., and Beckwith, J. (1995) Tight regulation, modulation, and high-level expression by vectors containing the arabinose P-bad promoter, *J. Bacteriol. 177*, 4121−4130.
29. Schloss, J. V., Phares, E. F., Long, M. V., Norton, I. L., Stringer, C. D., and Hartman, F. C. (1979) Isolation, characterization and crystallization of RuBP carboxylase from autotrophically grown *Rhodospirillum rubrum*, *J. Bacteriol. 137*, 490−501.
30. Pellicer, M. T., Nunez, M. F., Aguilar, J., Badia, J., and Baldoma, L. (2003) Role of 2-phosphoglycolate phosphatase of *Escherichia coli* in metabolism of the 2-phosphoglycolate formed in DNA repair, *J. Bacteriol. 185*, 5815−5821.
31. Lord, J. M. (1972) Glycolate oxidoreductase in *Escherichia-coli*, *Biochem. Biophys. Acta 267*, 227.
32. Baba, T., Ara, T., Hasegawa, M., Takai, Y., Okumura, Y., Baba, M., Datsenko, K. A., Tomita, M., Wanner, B. L., and Mori, H. (2006) Construction of *Escherichia coli* K-12 in-frame, single-gene knockout mutants: the Keio collection, *Mol. Syst. Biol. 2*, Article 2006.0008.
33. Andrews, T. J., and Lorimer, G. H. (1987) Rubisco: Structure, mechanisms, and prospects for improvement, in *The Biochemistry of Plants: A Comprehensive Treatise, Vol. 10, Photosynthesis* (Hatch, M. D., and Boardman, N. K., Eds.) pp 131−218, Academic Press, New York.
34. Knight, S., Andersson, I., and Brändén, C.-I. (1990) Crystallographic analysis of ribulose 1,5-bisphosphate carboxylase from spinach at 2.4 Å resolution. Subunit interactions and active site, *J. Mol. Biol. 215*, 113−160.
35. Hartman, F. C., and Harpel, M. R. (1994) Structure, function, regulation, and assembly of D-ribulose- 1,5-bisphosphate carboxylase/oxygenase, *Annu. Rev. Biochem. 63*, 197−234.
36. Laing, W. A., and Christeller, J. T. (1976) A model for the kinetics of activation and catalysis of ribulose 1,5-bisphosphate carboxylase, *Biochem. J. 159*, 563−570.
37. Schneider, G., Lindqvist, Y., and Lundqvist, T. (1990) Crystallographic refinement and structure of ribulose-1, 5-bisphosphate carboxylase from *Rhodospirillum rubrum* at 1.7 Å resolution, *J. Mol. Biol. 211*, 989−1008.
38. Andersson, I. (1996) Large structures at high resolution: The 1.6 Å crystal structure of spinach ribulose-1,5-bisphosphate carboxylase/oxygenase complexed with 2-carboxyarabinitol bisphosphate, *J. Mol. Biol. 259*, 160−174.
39. Lundqvist, T., and Schneider, G. (1991) Crystal structure of activated ribulose-1,5-bisphosphate carboxylase complexed with its substrate, ribulose-1,5-bisphosphate, *J. Biol. Chem. 266*, 12604−12611.

BI700820A